JOC Article

Conformationally Controlled Intramolecular Charge Transfer Complexes

Daniel Kost,*,† Na'ama Peor,† Gali Sod-Moriah,† Yifat Sharabi,† David T. Durocher,‡ and Morton Raban‡

Department of Chemistry, Ben Gurion University of the Negev, Beer-Sheva 84105, Israel, and Department of Chemistry, Wayne State University, Detroit, Michigan 48202

kostd@bgumail.bgu.ac.il

Received March 8, 2002

Trans-1-acceptor-2-donor-substituted cyclohexanes (**1**), as well as their 4- (or 5-)methyl-substituted homologues (**2**), have been prepared and are shown to form intramolecular charge-transfer (donor−acceptor) complexes. These weak complexes are turned on and off by the chair−chair interconversion of the cyclohexane ring. The CT absorptions have been measured and the equilibrium constants for the ring reversal have been determined by UV/vis spectroscopy at 298 K, as well as by NMR spectroscopy at two temperatures: at 183 K, by direct comparison of signals due to the two chair conformations, and at 300 K, by comparison of calculated and measured widths of the α-proton signals. The Gibbs free energies assigned to the donor−acceptor interactions range between 0 and −1 kcal mol^{-1}. A crystal structure of one of the complexes (**1b**) confirms the intramolecular donor−acceptor alignment and interaction. The regioisomers of the methyl-substituted complexes were characterized by NOE interaction between the methyl and an α-proton cis to it.

Introduction

Intermolecular charge transfer (CT) complexes arising from the interaction of aromatic π-donor and acceptor molecules have been studied extensively.[1] Far fewer intramolecular CT analogues have been reported, primarily of the cyclophane type, in which the donor and acceptor portions are locked together in a rather rigid arrangement.[2] More flexible intramolecular CT complexes have been reported in a recent communication, whereby a cyclohexane skeleton is substituted at adjacent trans positions with aromatic donor and acceptor groups (**1**).[3] The appearance of a weak new absorption band in

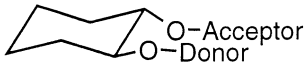

1

the UV/vis spectra of these materials, relative to the spectra of the separate donor and acceptor groups, provided evidence for the formation of an intramolecular CT complex.

In the present paper we describe the preparation and spectroscopic study of a series of analogous *trans*-1-acceptor-2-donor-cyclohexane (**1**) molecules, and their 4-(or 5-)methyl-substituted analogues (**2**, **2′**). UV/vis and NMR spectroscopies are utilized to measure the CT complex strengths and spectroscopic properties.

The cyclohexane ring system is known to undergo rapid chair−chair interconversion (eq 1). This dynamic process

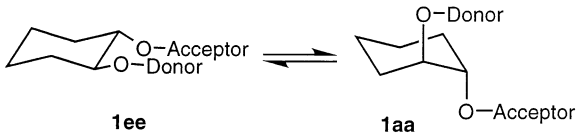

1ee **1aa** (1)

causes the donor and acceptor moieties to be either relatively far from each other in the diaxial geometry (**1aa**) or near each other in the diequatorial conformation (**1ee**). In the former, the substantial distance between the donor and acceptor rings prevents CT interaction and formation of an intramolecular complex; in the latter, however, the inter-ring distance is small enough and the geometry favorable to permit the formation of a CT complex.[4]

After the first demonstration of conformationally controlled intramolecular complexes,[3] it became of interest to evaluate the complex strengths, measure the molar extinction coefficients, and study possible substituent effects on complex properties: strength, λ_{max}, and ϵ. The long-range goal of this project is to develop on−off-

† Ben Gurion University.
‡ Wayne State University.

(1) (a) Foster, A. *Organic Charge-Transfer Complexes;* Academic Press: New York, 1969. (b) Mulliken, R. S.; Person W. B. *Molecular Complexes;* Wiely, New York, 1969. (c) Abdel-Kader, M. H.; Issa, R. M.; Ayad, M. M.; Abdel-Mottaleb, M. S. *Z. Naturforsch* **1984**, *39a*, 1274. (d) Bundi, M. L.; Jayadevappa, E. S. *Spectrochim. Acta* **1988**, *44A*, 607.

(2) (a) Cram, D. J.; Reeves, R. A. *J. Am. Chem. Soc.* **1958**, *80*, 3094. (b) Cram, D. J.; Bauer, R. H. *J. Am. Chem. Soc.* **1959**, *81*, 5971. (c) Cram, D. J.; Wilkinson, D. L. *J. Am. Chem. Soc.* **1960**, *82*, 5721. (d) Staab, H. A.; Krieger, C.; Wahl, P.; Kay, K.-Y. *Chem. Ber.* **1987**, *120*, 551.

(3) Preliminary results were communicated: Raban, M.; Durocher, D. T. *Tetrahedron Lett.* **1990**, *31*, 5125.

(4) This assessment has been tested and verified recently by a theoretical study: Kost, D.; Frailich, M. *Theochem J. Mol. Struct.* **1997**, *399*, 265.

10.1021/jo020164t CCC: $22.00
Published on Web 09/07/2002

CHART 1

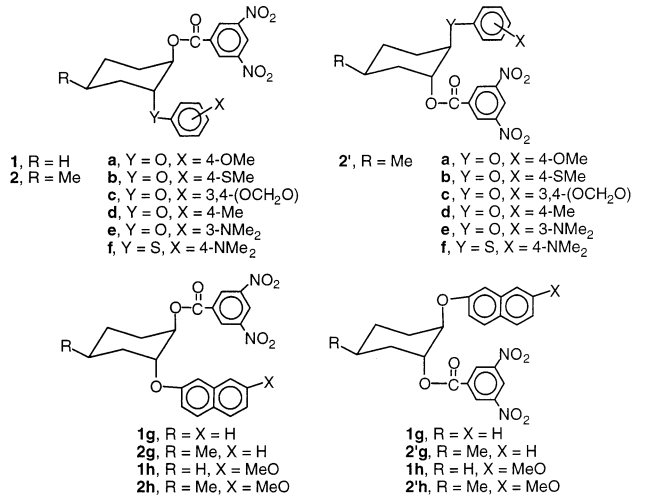

switchable CT complexes that will function as color indicators for molecular switches. The requirements from such CT complexes are that their absorptions fall well within the visible range and at significant absorptivities.

Methods

The chair−chair equilibrium reaction of the cyclohexane ring can be utilized to study the complex strength, by comparison between complexes of type **1** with their methyl-substituted analogues **2** (Chart 1). In series **1**, the equilibrium is shifted predominantly toward the **1ee** conformation, because both of the factors present, steric and CT interaction, favor this conformation. In dilute solution, CT interaction is essentially all intramolecular (as will be shown below), and hence, the stoichiometric concentrations represent actual CT complex concentrations. The molar extinction coefficients of the CT complexes can therefore be evaluated directly from the absorbances and stoichiometric concentrations.

The introduction of a methyl substituent at the 4-position (**2**) strongly affects the equilibrium constant. The substantial preference of the methyl group to occupy an equatorial position partly offsets both the steric preference of the donor and acceptor substituents to occupy equatorial positions and the CT interaction. The equilibrium constant K_{eq}, which can be measured either by electronic or by NMR spectroscopy, can lead to the assessment of ΔG_{comp}, the free energy of the CT interaction, as follows:

$$\Delta G_{eq} = -RT \ln K_{eq} \qquad (2)$$

The free energy ΔG_{eq} is the sum of the free energy components resulting from the steric preferences of the three substituents and the complex-binding term ΔG_{comp} (eqs 3 and 4). The steric free energies are simply the steric *A* values for methyl, phenoxy, and benzoyloxy groups.[5]

$$\Delta G_{eq} = \Delta G_{comp} + \Delta G_{OPh} + \Delta G_{OCOPh} - \Delta G_{Me} = \Delta G_{comp} - A_{OPh} - A_{OCOPh} + A_{Me} \qquad (3)$$

SCHEME 1. Synthetic Route for CT Complexes (Shown for Benzene-Derived Donors)

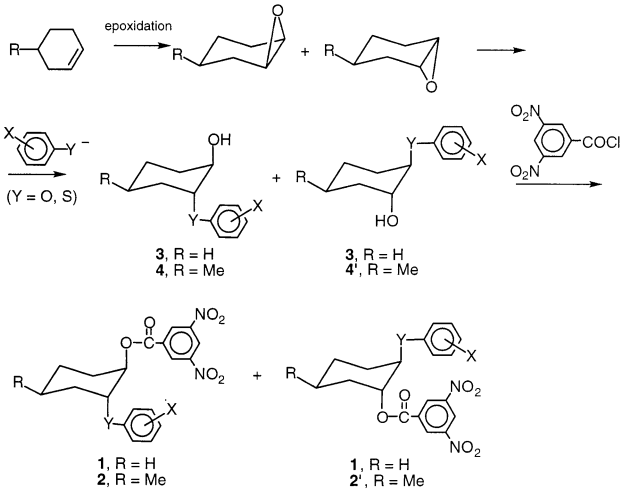

and hence

$$\Delta G_{comp} = \Delta G_{eq} + A_{OPh} + A_{OCOPh} - A_{Me} = \Delta G_{eq} + 0.65 + 0.5 - 1.74 = \Delta G_{eq} - 0.59 \qquad (4)$$

Results and Discussion

(a) Synthesis. The general synthetic route leading to all of the complexes is shown in Scheme 1. Epoxidation using three different reagent systems (perbenzoic acid freshly prepared from benzoyl peroxide,[6] hydrogen peroxide in the presence of trichloroacetonitrile,[7] and *N*-bromosuccinimide[8]) proceeded with essentially the same results: yields between 60 and 75% of a cis and trans mixture (for series **2**) of 4-methylcyclohexene oxide. The mixtures were further reacted with substituted phenolates or thiophenolates, producing nearly equal amounts of the regioisomers (**4** and **4′**) resulting from axial attack on the epoxides. The overall 1,2-trans (in **3**, **4**, and **4′**) and 1,4-cis (in **4**, 2,5-cis in **4′**) stereochemistry was obtained exclusively in all cases.

The mixtures of regioisomer pairs **4** and **4′** were separated to their individual components in three cases (**4a**, **4′a**; **4b**, **4′b**; and **4d**, **4′d**) by fractional crystallization from ethyl acetate/*n*-hexane mixtures. All other cyclohexanols **4** were further used as mixtures, from which regioisomeric CT complex mixtures, **2** and **2′**, were obtained and studied as mixtures. Conversion of **3**, **4**, and **4′** to **1**, **2**, and **2′** proceeded smoothly by reaction with 3,5-dinitrobenzoyl chloride.

(b) Characterization of Regioisomers. Identification of the regioisomers **2** and **2′** was accomplished by observation of a nuclear Overhauser enhancement (NOE) between the methyl group and the α-proton in position 3 relative to it. Examination of the conformations in Scheme 2 reveals that in the **2ee** conformation the protons in the α-position to the oxygens assume axial positions. In this conformation, the axial methyl group

(5) Eliel, E. L.; Wilen, S. H. *Stereochemistry of Organic Compounds*; Wiley: New York 1994; p 695.
(6) Braun, G. *Org. Synth. Coll. Vol* I, 431.
(7) Arias, L. A.; Adkins, S.; Nagel, C. J.; Bach, R. D. *J. Org. Chem.* **1983**, *48*, 888.
(8) Craig, T. W.; Harvey, G. R.; Berchtold, G. A. *J. Org. Chem.* **1967**, *32*, 3743.

SCHEME 2. Proximity of α-Hydrogens to the Methyl Group in 2aa and 2ee[a]

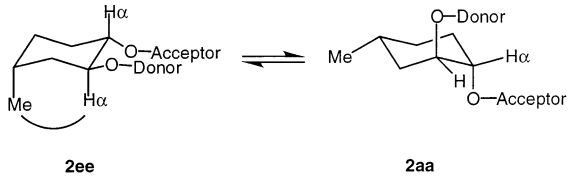

2ee **2aa**

[a] NOE expected only in **2ee**, between the methyl and the proton at position 3 to it.

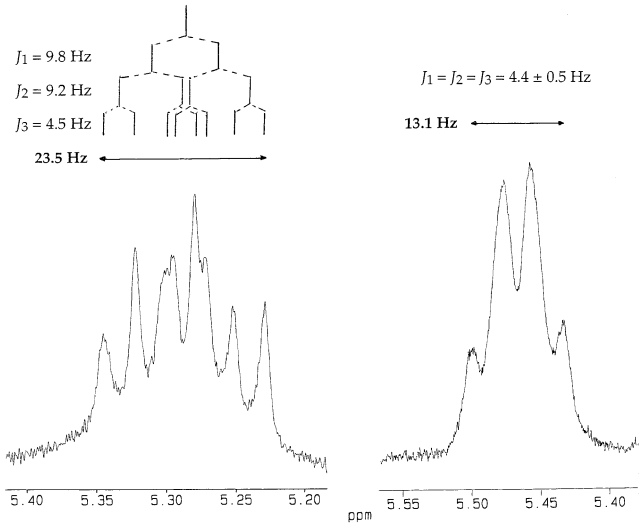

FIGURE 1. The α-proton region of the 200 MHz ^{1}H NMR spectra of **1b** (left) and **2b** (right).

is very close to the axial proton cis to it, in position 3 relative to the methyl. Consequently, selective low-power irradiation at the methyl resonance frequency should produce a NOE of the α-proton in the 3-position. This is borne out by NOE difference experiments (shown for complex **2′b** in the Supporting Information). The difference spectra show significant (4.4% for **2′b**) enhancement of the low-field (5.4 ppm) α-proton resonance, and proves that the acceptor group in this compound is in the 3-position relative to the methyl. In the corresponding regioisomer **2b**, in which the acceptor is in the 4-position relative to methyl, the NOE experiment results in a similar enhancement of the high-field proton α to the donor group.

This experiment was also run for the other pairs of isolated regioisomers **2a**, **2′a** and **2d**, **2′d**. It was concluded that in the **2** regioisomers the α-H resonances were the "inner" signals out of the total four (for both regioisomers), while the **2′** isomers gave rise to the "outer" signals (see the Supporting Information for sample NMR spectra).

(c) Conformational Analysis. The method is based, as mentioned earlier, on the assumption that the conformational equilibrium in series **1** is shifted predominantly toward the **1ee** conformation. Support for this initial expectation is found in the ^{1}H NMR signals of the α-protons in series **1**. Figure 1 shows the expanded region of the ^{1}H NMR spectrum for **1b**. Each α-proton has three vicinal neighboring protons that are spin-coupled to it. The magnitudes of the coupling constants depend on the molecular conformation in a Karplus-type relationship: if **ee** were the only conformation present, the α-protons would be axial and each one would be coupled to two axial and one equatorial neighbors. The maximum expected width of this multiplet would be 26.5 Hz, based on the sum of the three coupling constants, calculated for ideal 180° and 60° dihedral angles and taking into account the different substitution patterns for each proton [calculated: $^3J(H_\alpha H_\alpha) = 12.4$ Hz, $^3J(H_\alpha H_{\beta c}) = 2.8$ Hz, $^3J(H_\alpha H_{\beta t}) = 11.3$ Hz; these values are not significantly different for the sulfur-substituted compound **2f**].[9] In any other equilibrium situation the weighted average of **ee** and **aa** conformations would lead to significantly smaller coupling constants. Indeed, in all of the compounds of series **1** the α-proton multiplets are 24.0−25.5 Hz wide, corresponding to nearly exclusive occupation of the **ee** conformation, and thus justifying the assumptions.

In accord with this analysis, the widths of the α-proton signals of compounds of series **2** are substantially smaller (Figure 1), reflecting the much greater proportion of the **aa** conformation in these compounds due to the effect of the methyl group. For the pure **aa** conformation the three calculated coupling constants are 2.7−2.8 Hz,[9] and hence, the α-protons should give rise to a quartet of total width 8.2 Hz. The actual spectra for all but one pair of the compounds (**2f** and **2′f**) feature broad quartets or unresolvable multiplets for the α-protons, with a total width ranging between 13.1 and 14.5 Hz. From these bandwidths (W) the conformational equilibrium can be calculated using eq 5 (W_{ee}, J^{ee}, X_{ee} correspond to the calculated width of the quartet, calculated coupling constant, and mole fraction, respectively, of the ee conformation):

$$W = J_1 + J_2 + J_3 = (J_1^{ee} + J_2^{ee} + J_3^{ee})X_{ee} + (J_1^{aa} + J_2^{aa} + J_3^{aa})(1 - X_{ee})$$

$$X_{ee} = \frac{W - W_{aa}}{W_{ee} - W_{aa}} \qquad (5)$$

Substitution of the sums of calculated coupling constants in each conformation for W_{ee} and W_{aa}, respectively, and the measured spectral widths for W in eq 5 results in a range of $X_{ee} = 0.26-0.34$, corresponding to $0.35 < K_{eq} < 0.52$. It is concluded that, on the basis of coupling constants to the α-protons and on the modified Karplus equation, in all of the complexes **2** (except **2f**) the population of the uncomplexed conformation (**aa**) slightly exceeds that of the intramolecular CT complex (**ee**) conformation. In all of these complexes the width of the proton signal α to the donor fell within 1 Hz of the width of the proton signal α to the acceptor. Also, in both regioisomers (**2** and **2′**) these widths were equal, within experimental error.

For the pair **2f**, **2′f** the width of the α-multiplet (a doublet of triplets, $^3J(d) = 3.7$ Hz, $^3J(t) = 6.8$ Hz) was 17.3 Hz. Using eq 5 with this value yields $X_{ee} = 0.48$, i.e., $K_{eq} = 1$, corresponding to equal populations of the two conformations.

(9) The modified Karplus data are based on the following: Altona, C.; Francke, R.; Dehaan, R.; Ippel, J. H.; Daalmans, G. J.; Hoekzema, A. J. A. W.; Vanwijk, J. *Magn. Reson. Chem.* **1994**, *32*, 670, and references therein. We used a program for calculating ^3J values written by J. W. Blunt, University of Canterbury.

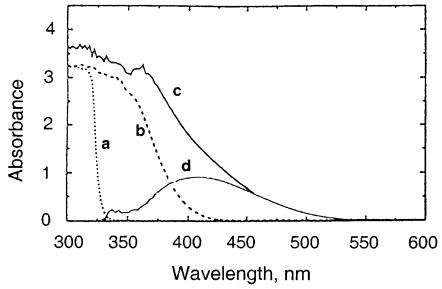

FIGURE 2. UV/vis absorption spectra of (a) **3b** (donor) and (b) ethyl 3,5-dinitrobenzoate (acceptor), 0.02 M of each in dichloromethane solution, and their mixture (c) resulting in CT complex **1b**; (d) the corresponding difference spectrum: donor and acceptor spectra subtracted from CT absorption (d = c − a − b).

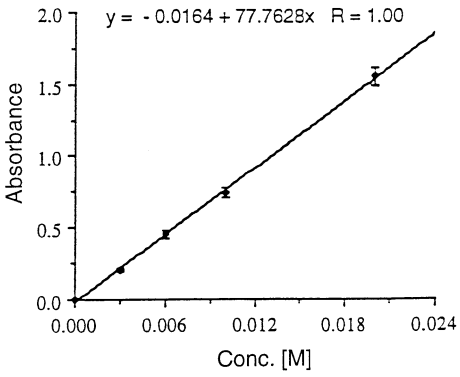

FIGURE 3. The absorbance of **1b** at λ_{max} in dichloromethane plotted against molar concentration.

(d) UV/Vis Spectroscopy. The CT absorption bands of the complexes of series **1** and **2** in the UV/vis spectra were measured as difference spectra, since there was substantial overlap between the relatively weak CT absorption and the strong end-absorptions of the donor and particularly the acceptor molecules (Figure 2). The difference was taken by subtracting the absorbances of ethyl 3,5-dinitrobenzoate and the appropriate donor molecule **3** from the absorption of the complex solution in the same solvent and concentration.

Determination of the extinction coefficients (ϵ) of the CT absorptions is based on the presumption that in compounds **1** the molecules are predominantly in the **1ee** conformation, and hence, CT concentrations can be expressed in terms of stoichiometric concentrations. Evidence to this effect was provided by the analysis of the NMR signals of the α-protons of compounds **1**, and additional evidence is presented in Figure 3: a linear correlation is obtained between the absorbance of each complex **1** and the concentration; i.e., within the given concentration range the CT absorptions obey Beer's law. It is therefore evident that no *inter*molecular complexation is present (which would be expected to depend on the concentration squared), and hence, all the absorbance is due to *intra*molecular complexation.

As a consequence, the ϵ values were evaluated for series **1** in a straightforward manner from the absorbances and concentrations and are listed in Table 1. It is assumed that in the **ee** conformation of both compounds **1** and **2** the CT interactions are very similar, and hence, the ϵ values measured for series **1** have been used for the corresponding complexes of series **2** to represent the absorptions of the **2ee** conformation.

TABLE 1. UV/Vis Absorption Maxima and Extinction Coefficients for Intramolecular CT Complexes 1 in CH_2Cl_2 Solutions

complex	λ_{max}, nm	ϵ, M^{-1} cm^{-1}	complex	λ_{max}, nm	ϵ, M^{-1} cm^{-1}
1a	380	60 ± 3	**1f**	480	410 ± 5
1b	388	72 ± 4	**1g**	366	166 ± 7
1c	382	68 ± 3	**1h**	370	244 ± 7
1e	434	227 ± 5			

The UV/vis spectra of series **2** served to evaluate the **aa** ⇄ **ee** equilibrium constants, K_{eq}. The absorbances of complexes **2** were substantially smaller than those of the corresponding **1** at equal concentrations, due to the effect of the methyl group in **2** to decrease the population of the **ee** conformation. Equilibrium constants, free energies of the conformational equilibrium, and the resulting binding free energies of the complexes (ΔG_{comp}) were determined as detailed in the Methods section and are listed in Table 2. The data in Table 2 show that in all of the complexes K_{eq} is smaller than 1, so that the CT interaction is not sufficiently strong to override the methyl steric preference. The only exception to this is **2g**, for which K_{eq} is significantly greater, although the donor group is not stronger than for other members of the series. This is probably the result of difficulties in obtaining accurate difference spectra for **2g**, since the overlap between absorption bands was more severe. In fact, for **2g** the λ_{max} value shifted with concentration, as a result of poor subtraction.

The UV/vis data in Tables 1 and 2 lead to the following conclusions: (a) in all the compounds **1** and **2** an intramolecular CT interaction is evident from the characteristic absorption and the associated color of the substance. (b) The complex binding energies are small but significant, generally between −0.2 and −0.5 kcal mol^{-1}. (c) Due to low resolution and difficulties in subtraction of the spectra, the error associated with this method may be substantial. (d) There is very good agreement between equilibrium constants measured by the UV/vis method and those estimated from the widths of the NMR signals of the α-protons (K_{eq} ranging between 0.35 and 0.52, except for **2f**, for which K_{eq} was 1.0). (e) The CT complex strengths do not depend critically on the donor strengths: all of the complexes fall within the same strength range.

The NMR results suggested that **2f** was a stronger CT complex than other compounds **2**. This is not borne out by the UV/vis results, possibly because of the inaccuracy of the latter, and remains an open question.

(e) Low-Temperature NMR Spectra. The two interconverting conformers **ee** and **aa** for each compound **2** and **2′** can be observed directly by NMR spectroscopy at low temperature, at which the exchange process is sufficiently slow with respect to the NMR time scale. An example of such a spectrum at 183 K, at which the exchange process has "frozen", is shown in Figure 4. Comparison of the various signal-pair intensities (by electronic integration as well as by cutting out and weighing the signals) provides the population ratio of the two conformers and hence the equilibrium constant. The K_{eq} values obtained in this manner for compounds **2** and **2′** are listed in Table 2. The best resolution to major and

TABLE 2. 2aa ⇄ 2ee Equilibrium Constants, Free Energies, and CT-Binding Free Energies for Series 2 from UV/Vis spectra at 298 K (CH_2Cl_2) and from ^{1}H NMR Spectra at 183 K (CD_2Cl_2)

	UV/vis data at 298 K			NMR data at 183 K		enthalpy and entropy[b]	
complex	K_{eq} = ee/aa	$\Delta G°$, kcal mol^{-1}	ΔG_{comp}, kcal mol^{-1}	K_{eq} = ee/aa	$\Delta G°$, kcal mol^{-1}	$\Delta H°$, kcal mol^{-1}	$\Delta S°$, cal mol^{-1} deg^{-1}
2a	0.68	0.23	−0.36	0.09 ± 0.02	0.88	1.9	5.6
2′a	0.58	0.32	−0.27	0.10 ± 0.01	0.84	1.7	4.5
2b	0.65	0.25	−0.34	0.13 ± 0.01	0.74	1.5	4.2
2′b	0.66	0.25	−0.34	0.13 ± 0.01	0.74	1.5	4.3
2c + **2′c**	0.62	0.28	−0.31				
2d				0.10 ± 0.02	0.84		
2′d				0.10 ± 0.02	0.84		
2e + **2′e**	0.33	0.66	0.07	0.15 ± 0.02	0.69	0.7	0.3
2f + **2′f**[a]	0.50	0.41	−0.18				
2g + **2′g**	1.88	−0.37	−0.96	**2g**: 0.46 ± 0.03	0.28	1.3	5.7
				2′g: 0.31 ± 0.05	0.43	1.7	6.9
2h + **2′h**	0.91	0.06	−0.53	**2h**: 0.36 ± 0.02	0.37	0.9	2.7
				2′h: 0.25 ± 0.03	0.50	1.2	3.9

[a] The resolution for **2f** + **2′f** at low temperature was insufficient to permit measurement. [b] Calculated from the two-temperature data.

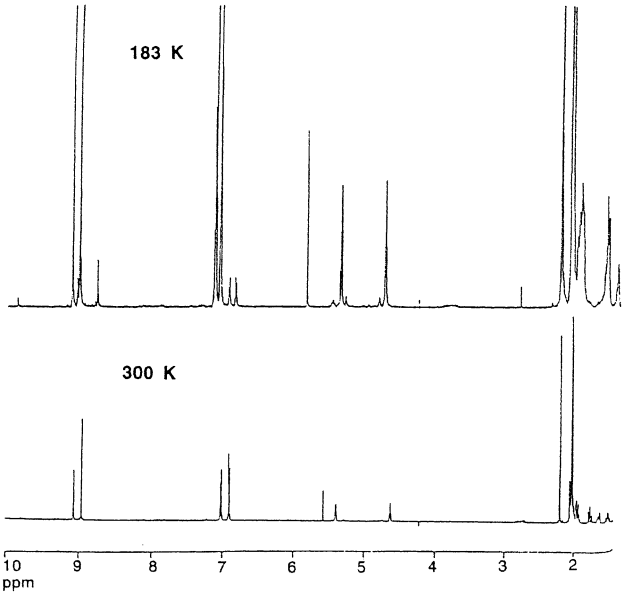

FIGURE 4. ^{1}H NMR spectra of **2d** in CD_2Cl_2 at 300 and 183 K, showing the "freezing out" of the conformational exchange.

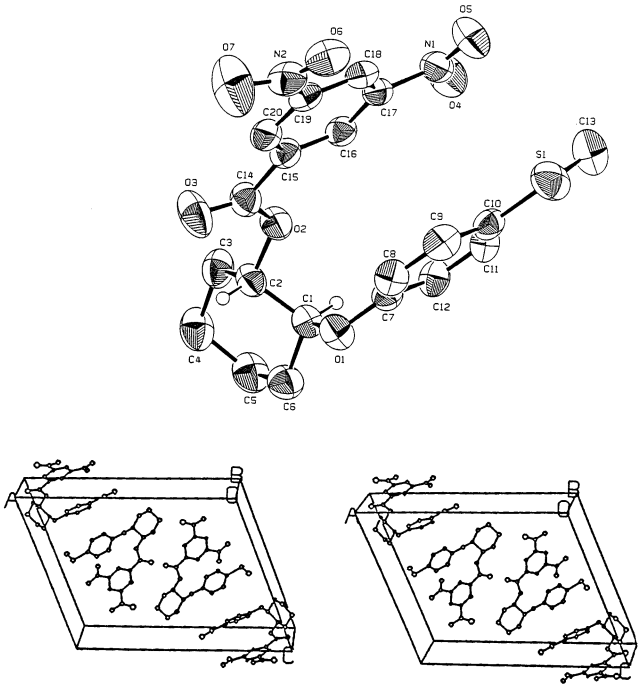

FIGURE 5. X-ray crystal structure of **1b** (orange polymorph) Top: molecular geometry. Bottom: stereoview of crystal packing.

minor isomer signals can be found in the aromatic protons of the *p*-tolyl ring (Figure 4). For other groups and other compounds, resolution was not always sufficient to permit determination of equilibrium constants. The best resolved signal pairs were chosen for the data in Table 2.

(f) Crystal Structure and Polymorphism. Upon recrystallization of **1b** from ethyl acetate/hexane, two different crystal forms (polymorphs) separated, one dark-orange with needlelike crystals, mp 102.4 °C, and the other one yellow and amorphous with cottonlike shape, mp 94.1 °C. The high melting polymorph was subjected to an X-ray crystallographic analysis, and its molecular geometry is depicted in Figure 5. The crystal structure clearly demonstrates that even in the solid-state intramolecular CT interaction is preferred over intermolecular interaction: the molecules are in the **ee** geometry, and the aromatic rings of one molecule are mutually perpendicular to those of the neighboring molecules, so that intermolecular interactions are practically excluded.

The mixture of the two forms of **1b** was subjected to a differential scanning calorimetry (DSC) measurement (Figure 6), which confirmed the expectation that these are two forms of the same material. Interestingly, the low-melting material slowly transformed upon standing at room temperature to the high melting (and darker) polymorph until, after a few weeks, it had completely disappeared.[10] Later recrystallizations no longer succeeded in producing this polymorph. From the less intense color it may be speculated that in the less stable polymorph the molecular geometry did not permit effective CT interaction. The geometry of this polymorph could possibly be the **aa** conformation, in which intramolecular

(10) The phenomenon of "disappearing polymorphs" is well-known and has recently been addressed in a review: Bernstein, J.; Dunitz, J. D. *Acc. Chem. Res.* **1995**, *28*, 193.

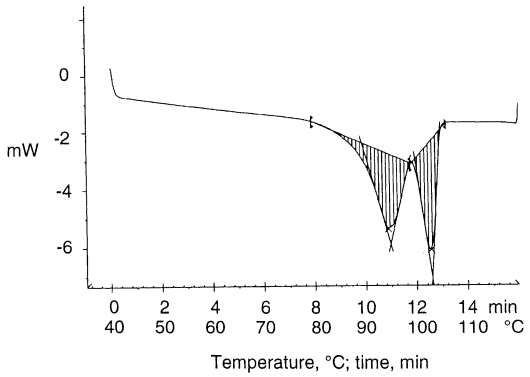

FIGURE 6. Differential scanning calorimetry (DSC) spectrum of a mixture of polymorphs of **1b**: heating rate, 5.00 °C min^{-1}; peak temperatures, 94.13 and 102.43 °C; extrapolated peaks, 94.57 and 102.67 °C.

interaction is impossible and in which intermolecular interactions may not be very intense, and hence the lighter color. However, it could equally well be a different crystal packing of the same (**ee**) molecular geometry. Crystallographic analysis of the low-melting polymorph could not be carried out to answer these questions, because no definite crystals had separated.

(g) Comparison of Results. The conformational equilibria at room temperature for compounds **2** are all close to 1, as determined both by the width of the ^{1}H NMR α-proton signals and by UV/vis spectroscopy. The resulting complex-binding energies, ΔG_{comp}, are small (around −0.5 kcal mol^{-1}) but negative; i.e., there is attractive interaction between the donor and acceptor groups. The equilibrium constants measured by NMR spectroscopy at 183 K are substantially smaller; i.e., at this temperature the population of the CT-bound **2ee** conformation is significantly lower. This obviously results from the large temperature difference. The two K_{eq} measurements made for each compound over a wide range of temperatures permit an estimate of the enthalpy and entropy for the conformational exchange reaction (eqs 6 and 7, derived from $-RT \ln K = \Delta H - T\Delta S$):

$$\Delta H° = \frac{R(\ln K_1 - \ln K_2)}{1/T_2 - 1/T_1} \quad (6)$$

$$\Delta S° = \frac{R(T_1 \ln K_1 - T_2 \ln K_2)}{T_1 - T_2} \quad (7)$$

The calculated $\Delta H°$ and $\Delta S°$ values are listed in Table 2. While obviously these are crude results, based on only two temperatures each, they nevertheless provide some insight to the complex formation: all of the complexes have small positive reaction enthalpies, which means that the complex strength is not sufficient to overcome the conformational preference of the methyl group. On the other hand, all of the complexes have small *positive* reaction entropies. The remarkable significance of the positive entropy is that it indicates that the CT-bound (**ee**) conformation has a higher entropy, and hence is *less* ordered, than the corresponding **aa** conformation. Indeed, at low temperature the unbound conformation is favored, since at lower temperature the enthalpy term becomes dominant. This may be rationalized in terms of the weak CT interactions that apparently operate between the molecules **2** and the solvent. Such solvent−solute interactions are more likely for the **aa** conformation, in which the donor and acceptor groups cannot interact with each other, and may be geometrically more exposed to contact with solvent molecules. The weak solvent−solute interactions involve substantial negative entropy. This is not as effective at low temperature as it is at high temperature, and as a result at low temperature this negative-entropy conformation becomes more populated.

Conclusion

Intramolecular, on−off-switchable CT complexes have been prepared and their complex strengths and spectral properties measured by UV/vis and NMR methods. The complexes had CT-binding energies in the range from −1 to 0 kcal mol^{-1}. In terms of effectiveness of the color as an indicator, **1f** and **2f** seem to be most suitable: their visible color is more intense because their CT absorption band is shifted to longer wavelength, and as a result, it is isolated from the acceptor and donor absorptions and can be measured more readily (without subtraction).

Acknowledgment. Financial support by the US−Israel Binational Science Foundation (BSF) is gratefully acknowledged.

Supporting Information Available: The Experimental Section, including synthetic procedures and characterization data for all of the compounds, is given in the Supporting Information, as well as details and data tables for the crystal structure determination of **1b**, and a ^{1}H NMR difference NOE spectrum for **2′b**. This material is available free of charge via the Internet at http://pubs.acs.org.

JO020164T